FLOW PATTERNS CAUSING INSTABILITIES IN THE PERFORMANCE CURVES OF CENTRIFUGAL PUMPS WITH VANED DIFFUSERS

by

Peter Hergt

Head, Central Department for Hydraulic Research and Development

and

Jörg Starke

Head, Department of Fluid Dynamics

Klein, Schanzlin & Becker AG

Frankenthal, West Germany

Peter Hergt is the Head of the Central Department for Hydraulic Research and Development of Pumps at Klein, Schanzlin & Becker AG (KSB), Frankenthal, West Germany.

He is responsible for all works concerning hydraulics as well as for the application of the results to the design and performance analysis of pumps. Included is the experimental and theoretical research on cavitation, efficiency improvement and performance stability.

Since joining KSB, he has been active in this field for 25 years. He has been awarded 10 patents in connection with pumps and has published 16 papers.

Mr. Hergt has a degree (Diplom Ingenieur) in Mechanical Engineering from the University of Karlsruhe, West Germany.

Jörg Starke received his engineering diploma in 1973 from the Technical University of Braunschweig, West Germany. During the following years he worked in the Institute of Fluid Mechanics (under former Director Prof. H. Schlichting) of the same University in the field of fluid mechanics and turbomachine aerodynamics.

In 1979, he completed his thesis on quasi-two-dimensional flows in compressor cascades.

After two years of research work on exhaust gas dust removal in the Bayer AG, Leverkusen, he joined Klein, Schanzlin & Becker AG, Frankenthal.

Mr. Starke presently is Head of the Department of Fluid Dynamics in the Central Department of Hydraulic Research.

ABSTRACT

It is well known that backflow regimes at the impeller inlet can lead to performance instabilities for centrifugal pumps at flowrates smaller than about 65 percent of the impeller inlet design flowrate. Performance curve instabilities can also occur at flowrates near the best efficiency point, i.e., at about 75 percent of the optimum flowrate. This is true for a special class of pumps, namely centrifugal pumps with vaned diffusers and specific speeds greater than 30 min^{-1}.

In connection with this type of instability, the axial forces are considerably changed, with the instability itself depending on manufacturing tolerances. A Reynolds-number effect, however, is not present.

The instability is caused by a very complicated three-dimensional flow structure inside the diffuser channels. The resulting backflow into the impeller is directed against the impeller rotation. Modifications of the diffuser vane leading edges based on two-dimensional flow models do not help to avoid the instability.

INTRODUCTION

In general, performance curve instabilities, or sudden deviations from the expected smooth performance curves of centrifugal pumps, should be avoided, due to the limitation such phenomena impose on the operating range of the pump. An instability, or local dent occurring very often, is due to a flow separation and a backflow regime in the impeller channels near the front disc. The flowrate at which the backflow regime appears in the impeller inlet section is about 65 percent of the *design* flowrate (design meaning the shockless entry of the flow). With further flowrate reduction, the backflow regime grows in the upstream direction as well as inwards from the pipe walls. It has a strong whirling motion and its blockage effect shifts the throughflow to a small zone around the pipe/pump axis. Because of this flow pattern, it is also called "part-load whirl" (PLW) [1,2,3]. The effects of the PLW on the performance characteristics are shown for a centrifugal volute pump with a specific speed $n_q = 85\ min^{-1}$ (Figure 1). At $Q/Q_{des} \approx 0.65$, the Q-H curve contains a distinct step towards smaller head values, although not an instability. Examples of instabilities can be found in the literature [1].

The PLW influences the incipient cavitation quantified by net positive suction head ($NPSH_i$). Starting from the design flowrate, the $NPSH_i$ increases with decreasing flowrate. At the PLW onset, there is a $NPSH_i$ maximum and a steep decrease with further flow reductions, due to the abrupt change in the flow pattern. Cavitation bubbles, if any, are visible at different locations along the impeller vanes. Without PLW, bubbles form at the outer diameter of the inlet, while with PLW, bubbles show up near the hub. A tremendous amount of research work has been dedicated to the PLW, [1,2,3] and some effective measures have been developed to counteract PLW and its consequences.

Very often performance curve dents or even instabilities are observed, which at first glance seem to have the same origin, and consequently are mixed with the PLW phenomenon. The situation shall be explained with the help of Figure 2, which contains the head and efficiency (Q-H and Q-η) curves for three

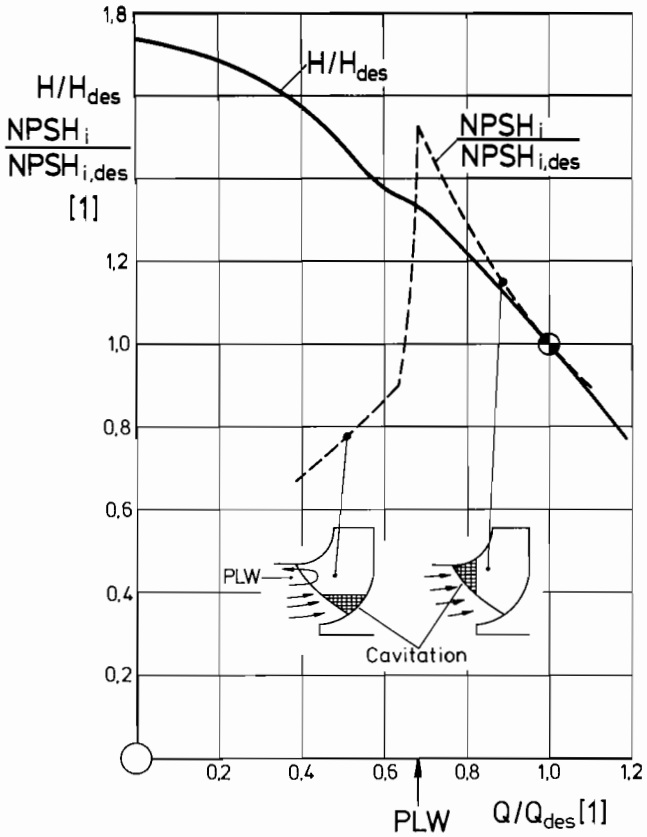

Figure 1. Performance Curve and Incipient Cavitation of a Centrifugal Pump with $n_q = 85\ min^{-1}$.

centrifugal pumps with different specific speeds, all equipped with vaned diffusers. For $n_q = 19\ min^{-1}$, no local deterioration of the performance can be seen. For $n_q = 30\ min^{-1}$, the typical step in the Q-H curve at small flowrates indicates the presence of a PLW. The corresponding Q-η curve remains smooth.

For $n_q = 35\ min^{-1}$, there is a distinct instability in the Q-H curve at more than 80 percent of the optimum flowrate, together with a local reduction of efficiency. In addition, a PLW seems to be present at smaller flowrates as well.

Similar results can also be found in the literature [4,5,6,7]. The generally important effect of the diffuser on the whole pump characteristic is emphasized by Kovats [8].

There is much evidence that this type of "full-load instability" (FLI) of the performance curves has its origin in a strong and very complicated backflow from the vaned diffusers. All of the pumps where such phenomena were found are equipped with this type of diffuser. The backflow itself is caused by relatively small disturbances of the impeller outlet flow at mild partload, which might also be connected with the flow patterns leading to the PLW. Closer inspection of experimental results reveals that the FLI generally occurs in vaned diffuser pumps with specific speeds greater than 30 min^{-1} at flowrates of more than 75 percent of the optimum flowrate. Conversely, FLI-like instabilities could not be observed in simple volute casing pumps. Only in Kovats' study [8] has a distinct kink of the Q-H curve been attributed to a flow separation on the diffuser vane suction side, due to too high diffuser divergence angles.

Because of the scarce knowledge of the full-load instability and its effects, a comprehensive, primarily experimental, program was initiated to clarify

- which overall characteristics of the pump were influenced by the flow patterns causing the FLI

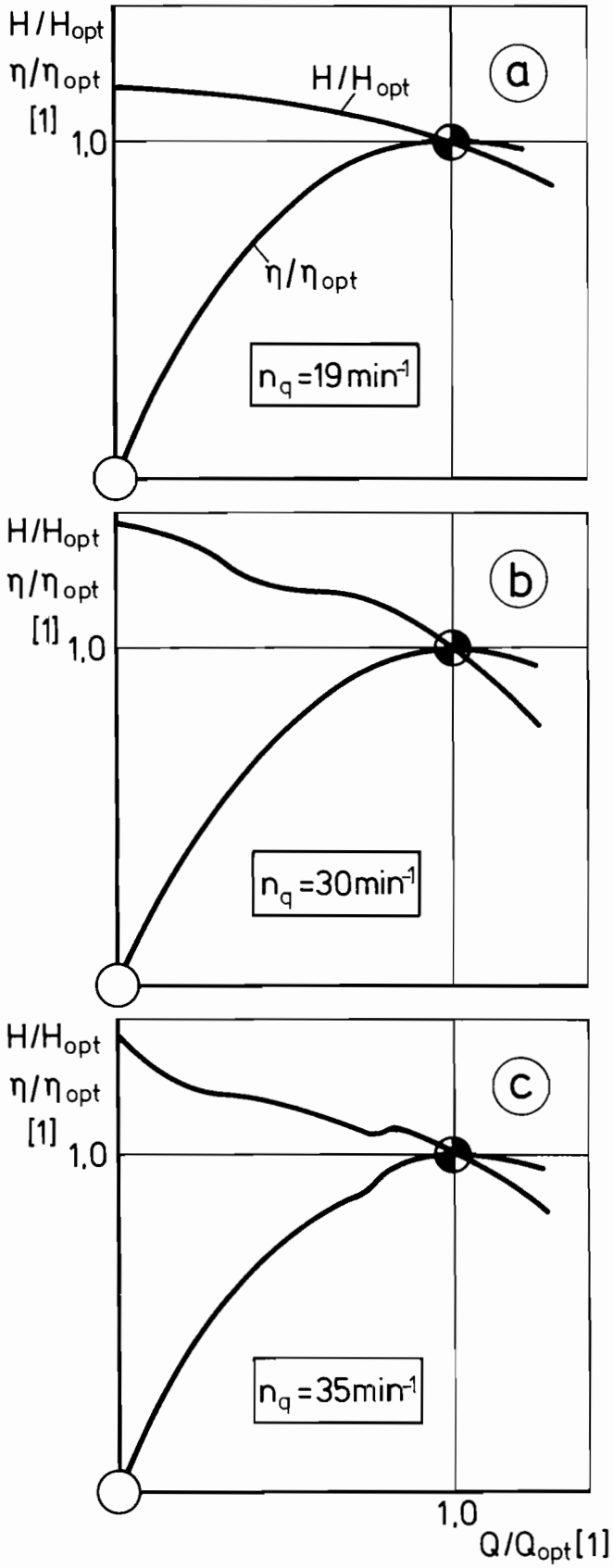

Figure 2. Influence of Specific Speed on the Shape of the Performance Curve a), b)—pumps, c) pump turbine.

- the main parameters which influenced the FLI
- the detailed flow patterns behind the impeller as well as inside the diffuser channels.

All these tasks were treated in parallel in different phases of the test program. The main results of the experimental investigations of the first phase are presented herein, along with a discussion of these findings.

OVERALL CHARACTERISTICS

As demonstrated with Figure 2, a distinct instability of the Q-H and the Q-η curves can occur in vaned diffuser pumps with n_q greater than 30 min^{-1}. Following the hypothesis made in the introduction, that the FLI is due to a backflow from the diffuser into the impeller, one also has to account for a possible effect on the flow in the lateral spaces of the impeller.

Measurements have been performed on a pump with $n_q = 45$ min^{-1} for static pressures in the lateral spaces. For the experiments, a standard test loop was used [9]. The pressures were measured with two pressure taps in the lateral spaces, at a radius corresponding to the outer diameter of the impeller. The results are shown in Figure 3. The Q-H curve has a similar shape, as in Figure 2, with the FLI starting at about 85 percent of Q_{opt}. A PLW seems to be present in further reduced part-load operation.

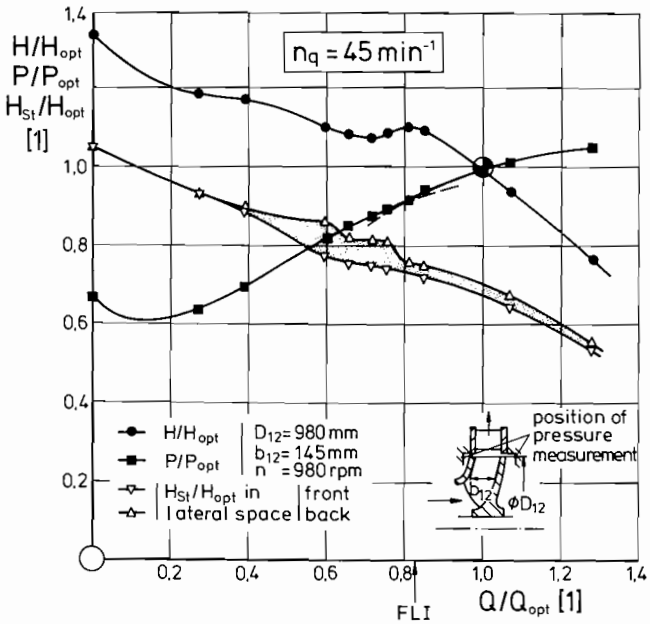

Figure 3. Performance Curve and Static Head in the Lateral Spaces of the Impeller.

The pressures in the lateral spaces start from the best efficiency point with a small difference resulting in an increase of the axial forces directed towards the impeller inlet. In the FLI region, the backwise pressure increases stepwise, and the front side pressure decreases more or less continuously. This necessarily leads to a jump of the axial force, which one would not expect normally. From 60 percent of Q_{opt} towards smaller flowrates, however, the pressures on both sides become continuously equal.

These findings are basically confirmed by on-site measurements on a $n_q = 30$ min^{-1} pump and demonstrate another very important feature of the flow pattern resulting in a FLI. The corresponding force measurements have been carried out for two axial positions of the impeller in comparison to the diffuser centerline (Figure 4). A shift of the impeller towards the suction side is represented as x = 0 mm, while x = 1.7 mm indicates a

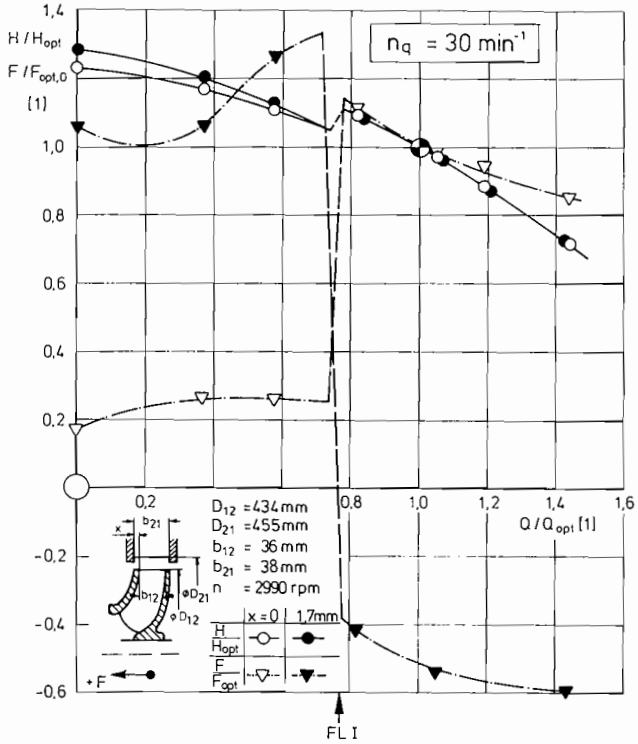

Figure 4. Performance and Axial Force Instabilities of Pump with a Vaned Diffuser.

shift towards the drive. Both Q-H curves are equivalent in the full-load region with a FLI at the same position. For smaller flowrates the curves diverge to a certain extent, with a maximum difference of five percent of H_{opt} at zero mass flow.

The two impeller positions, however, yield two extremely different axial forces. For x = 0, a positive force (directed towards the inlet) increases with decreasing flowrate. At the FLI onset, a sharp drop leads to values of 20 percent of the forces at the best efficiency point. For x = 1.7 mm, on the other hand, an overbalancing exists, yielding negative forces in the full-load region. At the FLI, there is an even sharper jump to large positive values. With respect to the force level in the x = 1.7 mm case, F_{opt} is also taken from x = 0 mm.

Referring again to Figure 3, a further interesting effect on the overall pumps characteristics is visible. At the FLI flowrate, there is also a discontinuity in the power input, with higher power consumption at flowrates below the FLI onset. One would expect this from extrapolation of the full-load power curve. Together with the strong head drop, this leads to a distinct drop in efficiency as shown in Figure 2.

These results drastically demonstrate that the flow patterns causing the FLI may cause further severe problems for the operation of the pump.

INFLUENCING PARAMETERS

It has been shown that the axial forces of a pump impeller are sensitive to the impeller position geometry, whereas the Q-H curve remains practically unchanged. The question that arises is whether or not the FLI itself also depends on *small* geometrical changes.

Additional experiments have been carried out in one of the standard test loops [9], where three diffusers cast from the same model were tested with the same impeller. The pump has a specified speed of 44 min^{-1}. Resulting basic data are given in Figure 5. For these tests, the position of the impeller with regard to the diffuser was carefully controlled.

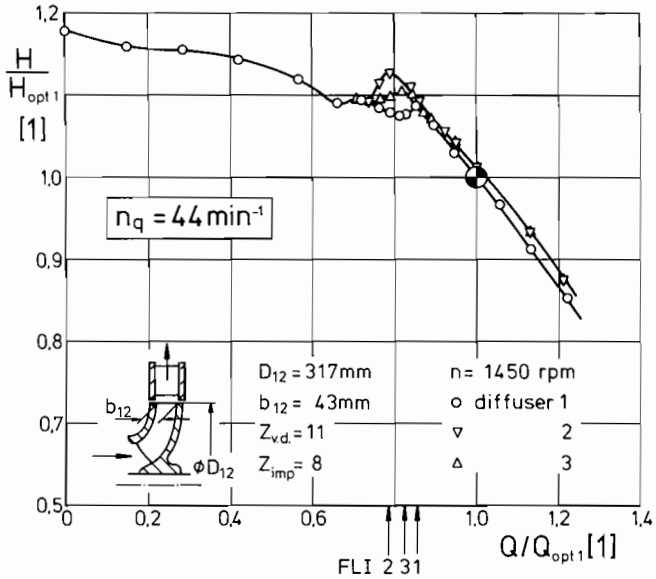

Figure 5. Influence of the Diffuser Manufacturing Tolerances on the Performance Curve.

The Q-H curves for flowrates smaller and greater than those in the FLI region are practically equivalent. Small differences in the full-load region do not exceed two percent of H_{opt}. In the FLI region, however, drastic changes are present for the three diffusers. The continuous series of the corresponding measuring points indicate that the differences in the Q-H values are not caused by a measurement uncertainty. Thus, the manufacturing tolerances, which in general are small enough to guarantee almost similar results for the greatest part of the performance curve, are too large for a critical part of the performance curve, unfortunately located near the best efficiency point. A basically similar result was described in Kovats [8], whereas only minor changes occurred in the multistage pump-turbine described by Amblard and Philibert [5]. However, Lazzaro and Rossi [4] reported that the gap between the impeller outlet and the diffuser vanes, as well as the form of the lateral spaces at impeller outlet, showed great influences on the performance. These facts should be taken into account if more than one pump has to be installed. During model testing of big machines, as well as tests with pumps operating in more than one fluid (for example, water and air), it should be kept in mind that tolerances can greatly affect performance.

When dealing with such tests, the influence of the Reynolds number also has to be known. On a standard test loop of the type described [9], Reynolds number tests were performed using a vaned diffuser pump with $n_q = 44$ min^{-1}. The Reynolds number was changed from $0.5(10^6)$ to $1.4(10^7)$ by varying the rotating speed from 100 to 2900 rpm. The Q-H curves are transformed to 2900 rpm and the FLI mass flowrate is determined as explained in Figure 6. Except for the points at $Re = 0.5(10^6)$, all the data did not vary significantly from a constant line at $Q/Q_{opt} \approx 0.75$. Therefore, one can conclude that the FLI position does not change within the range of realistic Reynolds numbers. Because the left most point was taken at 100 rpm, where a precise measurement was nearly impossible, this point should not be taken into account.

DETAILED EXPERIMENTAL INVESTIGATIONS

The primary results of the first phase of the measurements are described herein. These tests were performed at Reynolds numbers varying from $2.5(10^6)$ to $3.0(10^6)$. These values are located within the range of realistic Reynolds numbers (Figure 6).

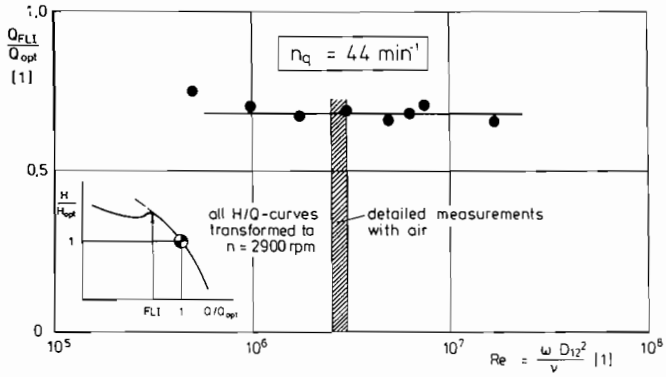

Figure 6. Effect of Reynolds Number on the FLI.

Test Rig, Measurement Technique and Experimental Program

The detailed flow measurements were carried out using air as the working fluid, thus simplifying the test facility and the measurement technique. The test rig is presented in Figure 7(a). Air enters the nozzle from the left and passes through a continuously adjustable throttle valve and a flow straightener. The pump is located on the right, and is driven through a belt by a constant speed electrical drive. The impeller rotating speed was 2380 rpm, giving a Reynolds number of $2.5(10^6)$. Details of the pump and the vaned diffuser are shown in Figures 7(b) and 7(c), respectively. The specific speed of the pump was about 30 min^{-1}. The air stream exits the diffuser directly into ambient air. Much care was taken to avoid any flow disturbance from outside sources, in order to keep the diffuser flow symmetrical. Therefore, the base of the pump was fitted with a number of slits which are not depicted in Figure 7(a).

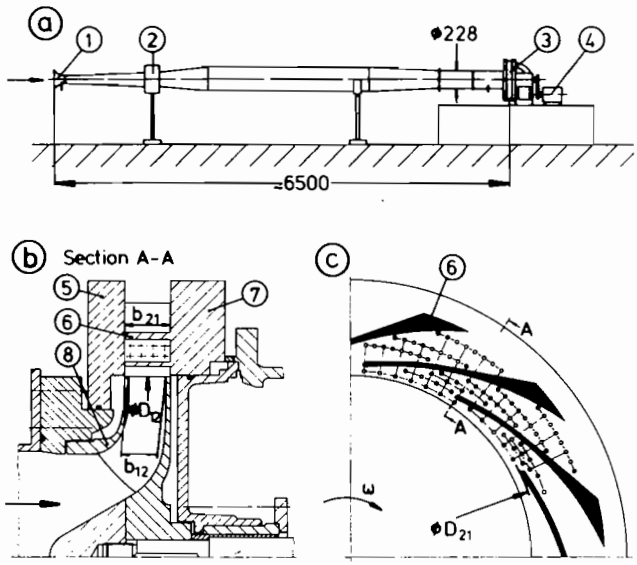

Figure 7. Test Rig for Detailed Flow Measurements. 1) quarter-circle nozzle, 2) throttle valve, 3) pump, 4) electric drive, 5) plexiglass front disc, movable, 6) diffuser vanes ($Z_{v.d.} = 12$), $D_{21} = 414$ mm, $b_{21} = 50$ mm), 7) aluminum back disk supporting the vanes, 8) impeller ($Z_{imp} = 7$, $D_{12} = 392$ mm, $b_{12} = 40$ mm, $\beta_{11\ hub} = 34°$, $\beta_{11\ cas} = 11°$, $\beta_{12} = 28°$).

The front disc of the diffuser was constructed of plexiglass with static pressure taps and holes for different probes and was movable in both the axial and circumferential directions. Pressure taps, as well as probe holes, were positioned along radial

lines covering the full extent of the diffuser and a small area in front of the diffuser.

The back diffuser disc supported the milled vanes and was equipped with static pressure taps distributed over three channels in order to yield a very high density of measuring points without manufacturing problems (Figure 7(c)). The radial distribution of the taps was the same as the distribution on the front disc.

On the vanes themselves, there were four lines of pressure taps as indicated in Figure 7 (b). Due to manufacturing problems, one vane was equipped with the pressure taps on the suction side, with another vane having taps on the pressure side. Thus, the taps were located inside one channel only.

The mass flow was determined with the nozzle, which had been previously calibrated. All pressures were measured with piezoresistive transducers.

In order to reduce the measuring expense, only the static pressure difference between impeller inlet and diffuser outlet was recorded. Although this method does not allow determination of the precise pump head, it was sufficient for determining the FLI.

The detailed measurements were performed with a hot wire probe and a Pitot probe for the velocities and total pressures, respectively. Both probes were inserted through the holes in the front disc and were movable in the axial direction. They could also be moved to any circumferential position by rotation of the disc.

In order to study the main flow parameters during the first phase, a very simple but reliable technique was used for both probes. The hot wire probe consisted of a single wire sensor at 90° to the probe axis. To determine the flow angles, the probe was rotated around the probe axis. The minimum output signal occurred when the wire was parallel to the flow, while the maximum signal occurred when the wire was perpendicular to the flow. At the same time, the hot wire indicated the flow velocity and turbulence [10]. The Pitot probe was of the kiel-type and was insensitive to flow angle variations which would have been expected behind the impeller [11].

The hot wire signals were processed by a standard hot wire instrumentation system yielding time averaged values. The kiel probe pressure signals were measured a piezoresistive pressure transducer. The whole pneumatic system was designed according to the recommendations of Johnson [12], in order to obtain true time averaged values.

The static pressures were determined basically in the same way as the probe pressures. The system utilized a pressure scanning controller to reduce the number of transducers involved during the testing.

All the analog signals were input into a central computer system via an analog-to-digital converter.

The experimental program was comprised of the performance curve measurements for the pump with the vaned diffuser, and detailed *velocity* and *total pressure* measurements in the flow field for four different mass flowrates chosen from the performance curve. Furthermore, some flow field measurements were performed using a vaneless-diffuser with a small radial extension (1.1 diameter ratio).

Performance Curve

The static head of the pump as the mass flowrate varied is shown in Figure 8. The optimum mass flow was taken from existing experimental results of the pump, using water as a working fluid. The FLI appeared at 75 percent of Q_{opt}. Detailed flow measurements were taken at ±5 percent of Q_{FLI}, i.e., at 71 percent and 79 percent of Q_{opt}, as well as at 100 percent and 121 percent of Q_{opt}.

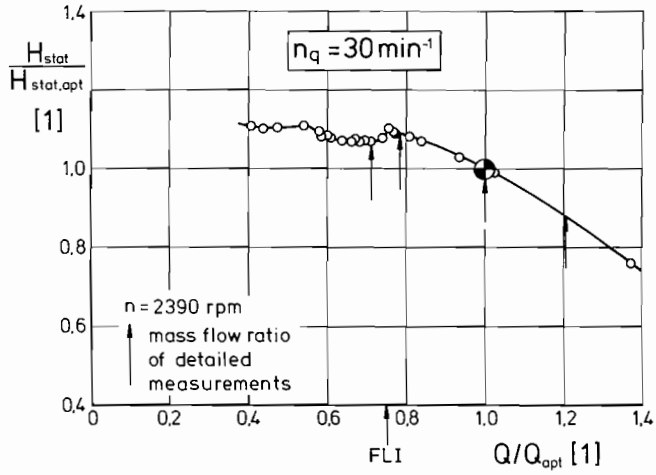

Figure 8. Performance Curve of Centrifugal Pump with Vaned Diffuser for Detailed Flow Measurements.

Velocities and Flow Angles in the Vaned Diffuser

The velocities in the r, θ-plane of the diffuser are shown in Figure 9. For clarity, only selected measured points have been shown in front of and inside the diffuser channel.

Vectors at $x_{v.d.}/b_{21} = 0.04$, 0.6 and 0.96 are shown in Figure 9(a) and (b) for the mass flowrates of 100 percent and 121 percent Q_{opt}, respectively. The distance $x_{v.d.}$ was measured from the front plexiglass disc.

At 100 percent Q_{opt}, there was little change in the vector length and angle along the diffuser width b_{21}. The flow through the channel was well-ordered, but near the front disc there was a small amount of backflow towards the impeller. Throughout the front disc boundary layer, the kinetic energy is lower than in the back disc boundary layer. Principally, the same was true for 121 percent Q_{opt}. It is interesting to note that even in the optimum and overload condition, the front disc suffered from low energy fluid and that a small backflow was already present.

Vectors in the same $x_{v.d.}/b_{21}$ planes for 79 percent Q_{opt} are shown in Figure 9(c). In this case, the flow was no longer well-ordered. Only at $x_{v.d.}/b_{21} = 0.60$ are the vectors similar in length and angle when compared to those of the previous figures. Near the back wall there was little throughflow and the flow was directed towards the vane pressure side. However, the backflow towards the impeller was weak. Near the front disc, very little throughflow was present any more. In the vane semi-section in front of the throat, the flow was turned back into the impeller with appreciably higher velocities being directed in the impeller rotation direction.

A deeper insight into the boundary layer flow is given in Figures 9(d) and 9(e), where the vectors at $x_{v.d.}/b_{21} = 0.04$, 0.1, and 0.2 and 0.8, 0.9, and 0.96, respectively, are depicted. It can be clearly seen that near the front disc, almost up to $x_{v.d.}/b_{21} = 0.2$, there was nearly no throughflow in half of the channel at the vane pressure side. In the vane mid-section, a great twist of the boundary layer flow can be seen, expecially near the vane leading edges.

On the contrary, the flow near the back disc seemed to be well-ordered. Although there was reduced throughflow in comparison to the mid-width, the vectors in the three $x_{v.d.}/b_{21}$ planes are nearly parallel. The vane-leading edge disturbing effect was considerably smaller.

Figure 9(f) contains the vectors for 71 percent Q_{opt}, which was already in the FLI-region. Again, the same three planes are shown as in Figure 9(c). In this case, the differences of planes $x_{v.d.}/b_{21} = 0.6$ and 0.96 had become much smaller in compari-

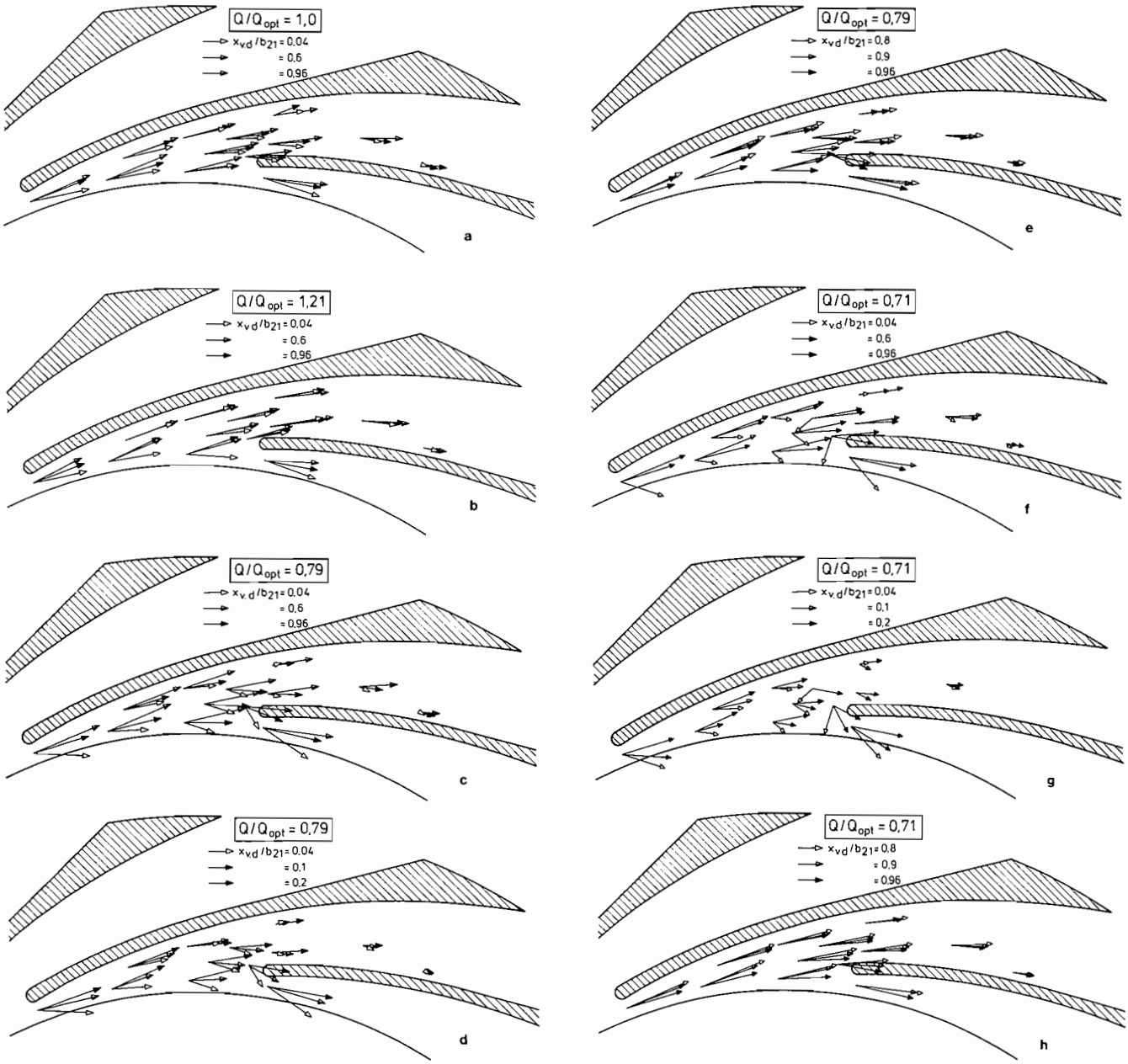

Figure 9. Velocity Vectors in the Diffuser Channels (a, b, c, d, e, f, g, h).

son to Figure 9(c), whereas near the front wall there was practically no throughflow any more. The backflow had become much stronger, with the mass flowing back coming from a large area around the vane leading edge and extending even behind the throat. In addition, it is worth noting that in this case the backflow was directed *against* the impeller rotation.

Considering the planes $x_{v.d.}/b_{21} = 0.04$; 0.1 and 0.2 in Figure 9(g) and $x_{v.d.}/b_{21} = 0.8$; 0.9 and 0.96 in Figure 9(h), basically the same statements about Figures 9(d) and 9(e) can be made. The only difference is that the flow patterns in comparison to 79 percent Q_{opt} were much more pronounced, i.e., the boundary layer twist was greater at the front wall, and the boundary layer was thicker. At the back disc, however, the flow was even more ordered than before. The boundary layer was thin and little disturbance was visible.

Backflow regimes in the impeller rotation direction at $Q > Q_{FLI}$ can also be found in pumps with smaller specific speeds, as was demonstrated for a pump with $n_q = 24$ min^{-1} [3]. In this case, however, no FLI was detectable.

Backflow regimes at the discs of the forementioned kind are a common feature of vaned diffusers in compressors [14]. In one study [14], the diffuser inlet flow was not created by an impeller, but by a special radial cascade adjusted in such a way that the flow was steady with constant properties in the axial and circumferential directions. The diffuser effect on the performance characteristics of the compressor, unfortunately, was not investigated.

Gorgidzhanjan and Ivanov [15] described bascially the same findings for a pump with $n_q = 30$ min^{-1}. Very detailed measurements inside the diffuser channels showed that at flowrates greater than 75 percent of Q_{opt}, a backflow was present at the front disc and was directed against the impeller rotation direction. Obviously, the backflow regime was located at the pressure side of the vane as was found in the experiments

described herein. Unfortunately, no performance curve information was given.

The impeller outlet flow leading to the diffuser flow patterns described is shown in Figures 10(a) and 10(b). The measurements were performed using a vaneless diffuser instead of the vaned diffuser. Naturally, the impeller outlet flow will be changed considerably through the vaned diffuser—especially in the FLI region. The results of Figure 10 represent only the potential flow, i.e., the flow provided by the undisturbed impeller.

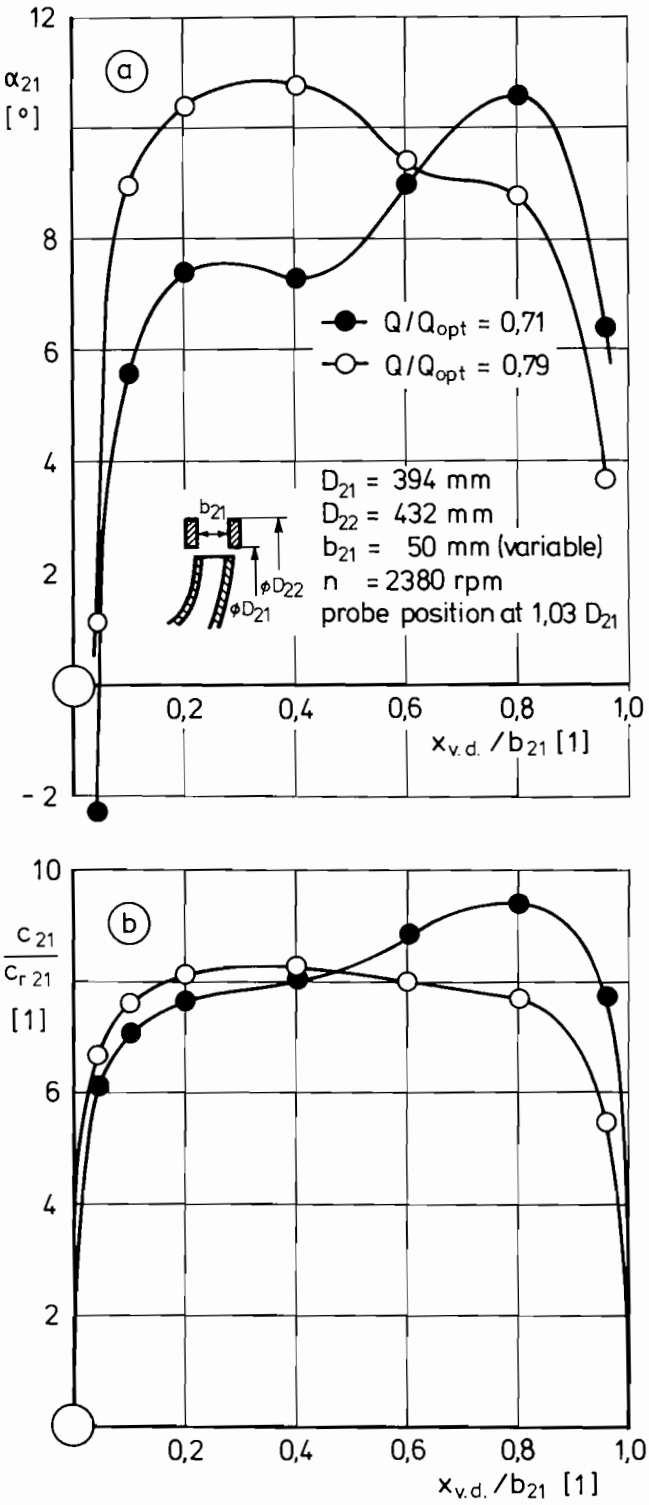

Figure 10. Flow Angle and Velocity Behind the Impeller with a Vaneless Diffuser.

For 79 percent Q_{opt} the α-variation along the diffuser width was about two degrees in the middle section, with higher flow angles near the front disc. The velocity change was about eight percent, again the higher values near the front disc. A sudden change in these flow patterns occurred with the mass flow reduction to 71 percent Q_{opt}. The values near the front disc were smaller, the angle change was about three degrees and the velocity change was about 20 percent.

These results converted into vectors are shown in Figure 11. There was a region near the front wall with nearly circumferential flow and smaller velocities, but neither the variation along the diffuser width nor the differences between the results for the two mass flowrates seemed to be very dramatic.

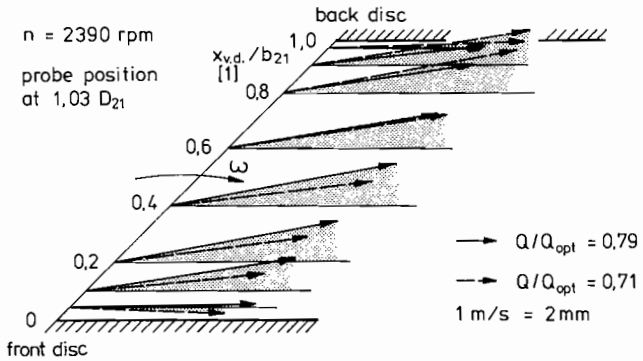

Figure 11. Velocity Vectors Behind the Impeller with a Vaneless Diffuser.

DISCUSSION

From the results presented, the following hypothesis can be derived. The FLI of a centrifugal pump with a vaned diffuser is due to the backflow regime in the diffuser channels being directed *against* the impeller rotation. The backflow itself, on the other hand, is due to a twisted impeller outlet flow. Near the front disc the flow angle is smaller than a critical flow angle, therefore a flow separation inside the diffuser channels occurs. Due to the small axial extension of the vanes as compared with the vane length and channel height, this separation influences the *whole* flow in the diffuser channels.

A similar type of axially varying flow quantities can also be found in compressors [16,17,18]. The amount of variation, however, is considerably greater than in pumps. In order to increase the compressor operating range, much effort has been dedicated to designing diffusers which tolerate greater flow variations along the axis [16,17,18,19,20].

One very interesting solution is the twisting of the diffuser vane leading edge [17,18]. For the compressor application, little improvement of the operating range was gained, but the efficiency was improved in a certain part of the operating range. The same solution applied to the pump of Figure 5 is shown in Figure 12. The diffuser vane leading edge was twisted up to about $-7°$ at the front disc and $+7°$ at the back disc. The result was rather disillusioning, because the new diffuser gave an even worse performance curve than the original diffuser. Although this kind of diffuser design admittedly was very rough, one fundamentally could conclude that the very complicated three-dimensional flow structure in the diffuser channels cannot be described with the common two-dimensional models.

CONCLUSION

Centrifugal pumps with vaned diffusers and specific speeds of more than 30 min^{-1} very often have a performance curve

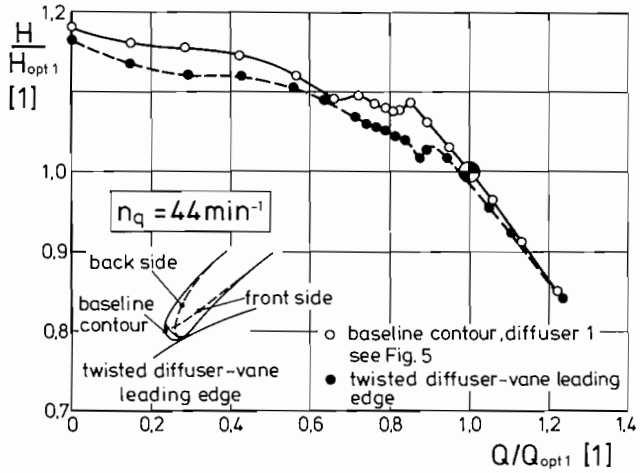

Figure 12. Influence of the Twisted Diffuser Vane Leading Edge on the Performance Curve.

instability near the best efficiency point. From experimental investigations, it has been shown that this instability is connected with a very sharp change in the axial force, which depends distinctly on the impeller axial position relative to the diffuser. The mass flowrate where the instability occurs varied considerably within the manufacturing tolerances, whereas little change with the Reynolds number was detected.

The instability is caused by a backflow region in the diffuser channel being directed against the impeller rotation. The backflow is due to an axial variation of the impeller outlet flow, which is characterized by small flow angles near the front disc.

A simple adjustment of the diffuser vane leading edge to this kind of flow angle yields an even greater instability. Thus two-dimensional flow models are not sufficient to describe the very complicated three-dimensional flow in vaned diffuser channels.

NOMENCLATURE

D [m]	diameter
b [m]	diffuser width
H [m]	head
n [rpm]	number of revolutions per minute
n_q [min^{-1}]	specific speed $n_q = n\sqrt{Q}/H^{3/4}$ n[rpm], Q [m^3/s], H [m]
NPSH [m]	net positive suction head
Q [m^3/s]	flowrate
r [m]	radial coordinate from pump axis
Re [1]	Reynolds number, $Re = \omega(D_{12})/\upsilon$
u [m/s]	peripheral speed
x [m]	axial coordinate, for impeller x = 0 at impeller front disc, for vaned diffuser x = 0 at diffuser front disc
Z [1]	blade number
α,β [°]	angle versus circumferential direction
θ [°]	circumferential coordinate from vertical line through pump axis
ν [m^2/s]	kinematic viscosity of the fluid
ω [1/s]	rotational frequency

SUBSCRIPTS

des	design
i	incipient cavitation
imp	impeller
opt	optimum = best efficiency point
stat	static
v.d.	vaned diffuser
12	impeller outlet
21	diffuser inlet
22	diffuser outlet

REFERENCES

1. Sen, M., "Prerotation in Centrifugal Pumps," VKI Lecture Series 978-3, *Off-Design Performance of Pumps* (1978).
2. Murakami, M. and Heya, N., "Swirling Flow in Suction Pipe of Centrifugal Pumps," Bull. JSME, *9*, (34), pp. 328-353 (1966).
3. Barrand, J. P., Caignaert, G., Canavelis, R., and Guiton, P., "Experimental Determination of the Reverse Flow Onset in a Centrifugal Impeller," *Proceedings of the First International Pump Symposium*, Texas A&M University, College Station, Texas, pp. 63-71 (1984).
4. Lazzaro, B. and Rossi, A., "Experimental Analysis of the Main Factors Affecting the Power of Hydraulic Machine Operating as a Pump at Zero Discharge," Proceedings of IAHR-Symposium on Operating Problems of Pump Stations and Power Plants, Amsterdam (1982).
5. Amblard, H. and Philibert, R., "Quelques Résultats de Recherches Concernant les Canaux de Retour des Turbines-pompes Multiétages," Proceedings of IAHR-Symposium on Operating Problems of Pump Stations and Power Plants, Amsterdam (1982).
6. Sutton, H., "Experience on Various Designs of Radial Diffuser Rings for Pump Application," BHRA Report No. RR. 154 (1972).
7. Clément, J. P., Quesnon, H., Deplanque, J. M., Lapray, J. F. and Philibert, R., "Incertitudes à Prendre en Compte sur les Courbes H(Q) et P(Q) à Débit Partiel des Pompes et de Pompes-Turbines," La Houille Blanche, *2/3*, pp. 123-129 (1982).
8. Kovats, A., "Effect of Non-Rotating Passages on Performance of Centrifugal Pumps and Subsonic Compressors," *Flow in Primary Non-Rotating Passages in Turbomachines*, H. J. Herring, et al. (eds.), ASME (1979).
9. "KSB Research and Development," KSB Separate Print No. 0500.03 E.
10. Raj, D. and Swim, W. B., "Measurements of the Mean Flow Velocities and Velocity Fluctuations at the Exit of an FC Centrifugal Fan Rotor," in *Measurement Methods in Rotating Components of Turbomachinery*, Lakshminarayana, B. and Runstadler, P., Jr., (eds.), ASME (1980).
11. Kiel, G., "A Total-Head Meter with Small Sensitivity to Yaw," NACA TM 775 (1935).
12. Johnson, R. C., "Averaging of Periodic Pressure-Pulsations by a Total Pressure Probe," NACA TN 3568 (1955).
13. Schrader, H., "Messungen an Leitschaufeln von Kreiselpumpen," Würzburg (1939).
14. Faulders, C. R., "Aerodynamic Design of Vaned Diffusers for Centrifugal Compressors," ASME paper No. 56-A-213 (1956).
15. Gorgidzhanjan, S. and Ivanov, V., "Flow Structure in the Channels of the Radial Vaned Diffuser of a Centrifugal Pump," (in Russian) Energetika, *6*, pp. 87-92 (1981).

16. Yoshinaga, J., Gyobu, I., Mishina, H., Koseki, F. and Nishida, N., "Aerodynamic Performance of a Centrifugal Compressor with Vaned Diffusers," in *Flow in Primary, Non-Rotating Passages in Turbomachines,* Herring, H. J., et al. (eds.), ASME (1979); also in Trans. ASME, Journal of Fluids Engineering, *102,* pp. 486-493 (1980).

17. Bammert, K., Jansen, M., Knapp, P. and Wittekindt, W., "Strömungsuntersuchungen an beschaufelten Diffusoren für Radial-verdichter," Konstruktion *28,* pp. 313-319 (1976).

18. Jansen, M., "Untersuchungen an beschaufelten Diffusoren eines hochbelasteten Radialverdichters," Ph.D. Dissertation, University Hannover (1982).

19. Anisimov, S., "Investigation of Two-Stage Vaned Diffusers of Centrifugal Compressors with Asymmetrical Blading," (in Russian) Izv. vuzov, Energ., *1,* pp. 96-99 (1983).

20. Senoo, Y., Hayami, H. and Ueki, H., "Low-Solidity Tandem-Cascade Diffusers for Wide-Flow-Range Centrifugal Blowers," ASME paper No. 83-GT-3 (1983).

ACKNOWLEDGEMENTS

The authors gratefully acknowledge the contributions of all the people involved in this project especially of Mr. J. Michelfelder and Mr. H. Lauer at Klein, Schanzlin & Becker AG in Frankenthal, West Germany. The permission for publication by KSB is greatly appreciated.